Received: 13 June 2023 | Accepted: 20 September 2023

DOI: 10.1002/pamm.202300010

PAMM Proceedings in Applied Mathematics and Mechanics

RESEARCH ARTICLE

Modelling of damage and failure within polymeric adhesives

Lukas Lamm[1] | **Jan Sistig**[1] | **Jan Mirco Pfeifer**[2] | **Hagen Holthusen**[1] | **Sebastian Felder**[1] | **Tim Brepols**[1] | **Stefanie Reese**[1]

[1]Institute of Applied Mechanics, RWTH Aachen University, Aachen, Germany

[2]Civil Engineering Mechanics, University of Wuppertal, Wuppertal, Germany

Correspondence
Lukas Lamm, Institute of Applied Mechanics, RWTH Aachen University, Mies-van-der-Rohe-Str. 1, 52074 Aachen, Germany.
Email: lukas.lamm@ifam.rwth-aachen.de

Funding information
AiF, Grant/Award Number: 21348 N/3; DFG, Grant/Award Numbers: 403471716, 404502442

Abstract

Within this contribution, we propose a fully thermo-mechanical coupled isotropic damage model for polymeric adhesives under finite strains. This model is based on the multiplicative decomposition of the deformation gradient into mechanical and thermal parts. We consider rate-dependent damage behaviour (e.g. creep damage) of the material by applying a Perzyna-type ansatz for the damage evolution equations. To overcome the pronounced mesh dependencies which would result from the usage of a local damage model, we make use of a gradient-extended damage formulation. Besides the main aspects of model, we show the thermodynamically consistent derivation of constitutive quantities as well as the numerical treatment of the governing equations. Finally, we show selected numerical examples to demonstrate the capabilities of the model.

1 | INTRODUCTION

Adhesive joints play a crucial role in many industrial applications. Their inherent advantages come with the drawback of a variety of inelastic, rate- and temperature-dependent material properties. The thermomechanical behaviour of polymer materials is nowadays considered to be very well studied (see e.g. [1] among others). From the numerical modelling side, the approaches developed can be roughly divided into two classes. One of these classes goes back to the work of the literature [2] in which the deformation is decomposed into a mechanical and a thermal part. The Helmholtz free energy is then divided additively according to these parts (see e.g. [1, 3]). On the other hand, there are approaches which do this without an explicit decomposition of the deformation gradient. Instead, they derive a corresponding energy equation by integrating the fundamental relationship between heat capacity and free energy (see e.g. [4]). This type of approach has the advantage that it is more general and can be reduced to the decomposition approach mentioned above under certain assumptions. In contrast to the decomposition approach, however, in the case of damage modelling it is not possible to ensure a priori that the damage growth criterion [5] is always fulfilled (see [6]). In this work, we therefore refer to the approach of multiplicative decomposition of the deformation gradient. Rate-dependent material behaviour is another important aspect that must be considered in the modelling of polymer materials. In addition to viscoelasticity, which has already been studied and modelled many times, rate-dependent damage effects also play a major role. The latter cannot usually be adequately represented by classical viscoelastic damage formulations within the framework of continuum damage theory. Various approaches to modelling the rate-dependent damage behaviour are known in the literature. A comprehensive overview would go beyond the scope of this paper. The interested reader is therefore referred to the overview for example in the literature [7, 8]. The approach of [8] uses a simple Perzyna approach [9] and forms the basis of the model presented here. Furthermore, it should be mentioned at this point that in the context of this work, modelling of the viscoelastic behaviour was dispensed with in order to study the influence of the rate-dependent damage on the thermomechanical material behaviour in more detail.

2 | CONTINUUM MECHANICAL MODELLING

We start by following the argumentation of the literature [2] to split the deformation gradient $\mathbf{F}$ into mechanical and thermal parts, such that $\mathbf{F} = \mathbf{F}_\theta \mathbf{F}_M$. For the thermal part, we assume that the material behaves isotropic under thermal expansion. This motivates the definition $\mathbf{F}_\theta = \vartheta(\Theta)\mathbf{I}$ using the heat expansion function $\vartheta(\Theta) = \exp(\alpha_\Theta(\Theta - \Theta_0))$, which is fully characterized in terms of the heat expansion coefficient α_Θ, the current temperature Θ and a reference temperature Θ_0. With defining the right Cauchy Green tensor $\mathbf{C} = \mathbf{F}^T\mathbf{F}$, we postulate the Helmholtz free energy of the given material as

$$\psi = f_d(D)\frac{\Theta}{\Theta_0}\psi_e(\mathbf{C}) + \psi_d(\xi_d) + \psi_{\bar{d}}(D, \bar{D}, \mathrm{Grad}\,\bar{D}) + \psi_\theta(\Theta). \tag{1}$$

Here, the damage local damage variable $D \in [0, 1]$ as well as its non-local counterpart $\bar{D}$ are introduced together with the damage hardening variable ξ_d. The damage degradation function is given as $f_d(D) = (1 - D)^2$. Whilst ψ_e describes the elastic energy contribution, ψ_d defines the energy contribution of damage hardening. Furthermore, $\psi_{\bar{d}}$ and ψ_θ denote the contribution with respect to the non-local damage formulation and the caloric energy, respectively. For the temperature dependence of the given energy, we use a linear relation as described for example in the literature [1].

2.1 | Thermodynamic considerations

In order to develop a thermodynamically consistent material model, we need to considering both, the balance of energy for a gradient-extended damage model as well as the corresponding Clausius-Duhem inequality. The former can be written in terms of the internal energy e, the second Piola-Kirchhoff stress tensor $\mathbf{S}$, the external heat sources r_{ext} as well as the generalized, micromorphic stresses a_{0_i} and $\mathbf{b}_{0_i}$, that is

$$\dot{e} = \mathbf{S} : \frac{1}{2}\dot{\mathbf{C}} - \mathrm{Div}\,\mathbf{q}_0 + a_{0_i}\dot{\bar{D}} + \mathbf{b}_{0_i} \cdot \mathrm{Grad}\,\dot{\bar{D}} + r_{ext}. \tag{2}$$

For the spatial heat flux $\mathbf{q}_0$, we need to consider that the virgin conductivity k_0 must be reduced during the damage process, which motivates the choice of $\mathbf{q}_0 = -f_d(D)Jk_0\mathbf{C}^{-1}\,\mathrm{Grad}\,\Theta$ [6]. Furthermore, the Clausius-Duhem inequality is expressed in terms of the bodies entropy η as

$$-\dot{\psi} + \mathbf{S} : \frac{1}{2}\dot{\mathbf{C}} + a_{0_i}\dot{\bar{D}} + \mathbf{b}_{0_i} \cdot \mathrm{Grad}\,\dot{\bar{D}} - \eta\dot{\Theta} - \frac{1}{\Theta}\mathbf{q}_0 \cdot \mathrm{Grad}\,\Theta \geq 0. \tag{3}$$

Considering a Legendre-Transformation $e = \psi + \Theta\eta$ and combining the temporal derivative of Equation (1) with Equations (2) and (3), we can find the thermodynamically consistent definition of the second Piola-Kirchhoff stress tensor, the entropy as well as the generalized micromorphic stresses as

$$\mathbf{S} = 2\frac{\partial\psi}{\partial\mathbf{C}}, \quad \eta = -\frac{\partial\psi}{\partial\Theta}, \quad \mathbf{b}_{0_i} = \frac{\partial\psi}{\partial\,\mathrm{Grad}\,\bar{D}}, \quad a_{0_i} = \frac{\partial\psi}{\partial\bar{D}}. \tag{4}$$

With this, the reduced Clausius-Duhem inequality is given as a function of the damage driving force Y and the hardening driving force q_d, that is

$$Y = -\left(\frac{\partial f_d}{\partial D}\frac{\Theta}{\Theta_0}\psi_e + \frac{\partial\psi_{\bar{d}}}{\partial D}\right), \qquad q_d = \frac{\partial\psi_d}{\partial\xi_d} \tag{5}$$

and can be written as $Y\dot{D} - q_d\dot{\xi}_d \geq 0$. In order to ensure thermodynamic consistency, the corresponding evolution equations for $\dot{D}$ and $\dot{\xi}_d$ must be chosen such that this inequality is always fullfilled. Additionally, the balance of energy can be reformulated such that it is described in terms of the internal heat generation r_{int} due to dissipation effects, that is

$$c\dot{\Theta} = r_{int} + r_{ext} - \mathrm{Div}\, \mathbf{q}_0. \tag{6}$$

These internal heat sources can be associated with elastic and damage related dissipation and therefore be written as $r_{int} = r_e + r_d$, where the individual heat production terms are given as

$$\begin{aligned} r_e &:= \frac{1}{2}\frac{\partial \mathbf{S}}{\partial \Theta}\Theta : \dot{\mathbf{C}}, \\ r_d &:= \left(Y - \frac{\partial Y}{\partial \Theta}\Theta\right)\dot{D} - \left(q_d - \frac{\partial q_d}{\partial \Theta}\Theta\right)\dot{\xi}_d + \frac{\partial a_{0_i}}{\partial \Theta}\Theta\dot{\bar{D}} + \frac{\partial \mathbf{b}_{0_i}}{\partial \Theta}\Theta \cdot \mathrm{Grad}\, \dot{\bar{D}}. \end{aligned} \tag{7}$$

Equation (6) describes the evolution of temperature over time and throughout the body of interest. Within the solution schema applied for this work, this equation has to be solved together with the balance of linear momentum in a coupled fashion.

2.2 | Evolution equations

To complete the constitutive relations described above, we further define appropriate evolution equations for the rate-dependent damage response. For this, we choose a scalar damage function which is defined in terms of the damage threshold Y_0, that is

$$\Phi_d := Y - (Y_0 + q_d). \tag{8}$$

Next, we introduce the damage multiplier $\dot{\lambda}_d$ and postulate the damage related evolution equations as

$$\dot{D} := \dot{\lambda}_d \frac{\partial \Phi_d}{\partial Y} = \dot{\lambda}_d \qquad \text{and} \qquad \dot{\xi}_d := -\dot{\lambda}_d \frac{\partial \Phi_d}{\partial q_d} = \dot{\lambda}_d. \tag{9}$$

It is important to note that this particular choice of the associative evolution equations yield the same result for both, the local damage variable D and the damage hardening variable ξ_d. Such an relatively simple approach is by no means the only feasible option, but has proven to be very effective. In the case of a classical rate-independent damage model, $\dot{\lambda}_d$ would serve as a Lagrangian multiplier which has to be solved using the Karush-Kuhn-Tucker conditions. In contrast to that, we introduce an explicit formulation for

$$\dot{\lambda}_d := \begin{cases} \eta_d \left(\frac{\Phi_d}{Y_0 + q_d}\right)^{\frac{1}{\varepsilon_d}} & \text{if} \quad \Phi_d \geq 0 \\ 0 & \text{else} \end{cases} \tag{10}$$

in order to introduce the temporal dependence into our model (see e.g. [9]). Here, η_d describes the damage velocity. Furthermore, ε_d is the so-called damage sensitivity parameter.

2.3 | Particular choice of the Helmholtz free energies

For simplicity reasons, we choose a classic Neo-Hookean type model as an elastic ground model for the material at hand, that is

$$\psi_e := \frac{\mu}{2}\left[\mathrm{tr}\left(J^{-\frac{2}{3}}\mathbf{C}\right) - 3\right] + \frac{\kappa}{4}\left(J^2 - 1 - 2\ln J\right), \tag{11}$$

with $J = \sqrt{\det \mathbf{C}}$ and μ, κ referring to the shear and bulk modulus of the material. It seems important to mention, that any other hyperelastic ground model is also feasible at this place.

For the energy density of the damage hardening contribution, we choose a combination of a Voce-type hardening (see [10]) and a classical linear hardening law including the material paramters k, r and s, that is

$$\psi_d(\xi_d) := \underbrace{\frac{1}{2}\, k\, \xi_d^2}_{\text{linear hardening}} + \underbrace{r\left(\xi_d + \frac{1}{s}[\exp(-s\xi_d) - 1]\right)}_{\text{Voce-type hardening}}. \tag{12}$$

Regarding the energy density of the micromorphic damage extension, we follow the choice of for example [11] or [12, 13] and define it such that

$$\psi_{\bar{d}}(D, \bar{D}, \nabla\bar{D}) := \frac{H}{2}(D - \bar{D})^2 + \frac{A}{2}\nabla\bar{D} \cdot \nabla\bar{D}. \tag{13}$$

Here, H acts as a penalty parameter to couple the local and non-local damage fields whereas A describes the influence of the non-local damage gradient.

By assuming that the heat capacity c is constant, we can neglect a explicit definition of the caloric energy ψ_Θ and assume that it takes a form for which this assumption is valid.

3 | ALGORITHMIC IMPLEMENTATION

The material formulation described above was implemented into the finite element program FEAP using a fully thermomechanical coupled, gradient-extended element formulation as described in the literature [6]. For this, the evolution equation given by (10) must discretized in time and solved appropriately afterwards. For this, we introduce $\Delta t = t - t_n$ and apply an implicit Euler method to Equation (9), that is

$$D = D_n + \Delta t\, \eta_d \left(\frac{\Phi_d}{Y_0 + q_d}\right)^{\frac{1}{\varepsilon_d}}, \tag{14}$$

where variables at the last time step are denoted by subscript n. To solve this discrete non-linear equation, we apply a local Newton Raphson iteration schema. The Jacobian $J_1 = \partial r/\partial D$ used for this are computed using automatic differentiation techniques instead of analytical derivations. This is achieved by using the automatic differentiation framework *AceGen* (see [14, 15]). With these at hand, we can determine the current value of the local damage variable D iteratively for the k − th iteration step via $D_{k+1} = D_k - J_1^{-1} r_k$. Since the local material response is implicitly included within the global material tangent operators of the finite element simulation, we need to derive these material sensitivities in a consistent manner. Otherwise quadratic convergence of the global iteration scheme can not be achieved. Due to the second Piola-Kirchhoff stress tensor $\mathbf{S}$ being a function of the right Cauchy-Green tensor $\mathbf{C}$, the non-local damage variable $\bar{D}$ as well as the temperature Θ and the internal variables, the tangent operators can be expressed as

$$\frac{\mathrm{d}\mathbf{S}}{\mathrm{d}\mathbf{C}} = \left(\left.\frac{\partial \mathbf{S}}{\partial \mathbf{C}}\right|_D + \left.\frac{\partial \mathbf{S}}{\partial D}\right|_{\mathbf{C}} : \frac{\partial D}{\partial \mathbf{C}}\right), \quad \frac{\mathrm{d}\mathbf{S}}{\mathrm{d}\Theta} = \left(\left.\frac{\partial \mathbf{S}}{\partial \Theta}\right|_D + \left.\frac{\partial \mathbf{S}}{\partial D}\right|_{\Theta} \frac{\partial D}{\partial \Theta}\right), \quad \frac{\mathrm{d}\mathbf{S}}{\mathrm{d}\bar{D}} = \left(\left.\frac{\partial \mathbf{S}}{\partial \bar{D}}\right|_D + \left.\frac{\partial \mathbf{S}}{\partial D}\right|_{\bar{D}} \frac{\partial D}{\partial \bar{D}}\right). \tag{15}$$

Similarly, the sensitivities of the internal heat sources, that is

$$\frac{\mathrm{d}r_{int}}{\mathrm{d}\mathbf{C}} = \left(\left.\frac{\partial r_{int}}{\partial \mathbf{C}}\right|_D + \left.\frac{\partial r_{int}}{\partial D}\right|_{\mathbf{C}} \frac{\partial D}{\partial \mathbf{C}}\right), \quad \frac{\mathrm{d}r_{int}}{\mathrm{d}\Theta} = \left(\left.\frac{\partial r_{int}}{\partial \Theta}\right|_D + \left.\frac{\partial r_{int}}{\partial D}\right|_{\Theta} \frac{\partial D}{\partial \Theta}\right), \quad \frac{\mathrm{d}r_{int}}{\mathrm{d}\bar{D}} = \left(\left.\frac{\partial r_{int}}{\partial \bar{D}}\right|_D + \left.\frac{\partial r_{int}}{\partial D}\right|_{\bar{D}} \frac{\partial D}{\partial \bar{D}}\right) \tag{16}$$

and the referential heat flux are given, that is

$$\frac{\mathrm{d}\mathbf{q}_0}{\mathrm{d}\mathbf{C}} = \left(\left.\frac{\partial \mathbf{q}_0}{\partial \mathbf{C}}\right|_D + \left.\frac{\partial \mathbf{q}_0}{\partial D}\right|_{\mathbf{C}} \otimes \frac{\partial D}{\partial \mathbf{C}}\right), \frac{\mathrm{d}\mathbf{q}_0}{\mathrm{d}\Theta} = \left(\left.\frac{\partial \mathbf{q}_0}{\partial \Theta}\right|_D + \left.\frac{\partial \mathbf{q}_0}{\partial D}\right|_{\Theta} \frac{\partial D}{\partial \Theta}\right), \frac{\mathrm{d}\mathbf{q}_0}{\mathrm{d}\bar{D}} = \left(\left.\frac{\partial \mathbf{q}_0}{\partial \bar{D}}\right|_D + \left.\frac{\partial \mathbf{q}_0}{\partial D}\right|_{\bar{D}} \frac{\partial D}{\partial \bar{D}}\right). \tag{17}$$

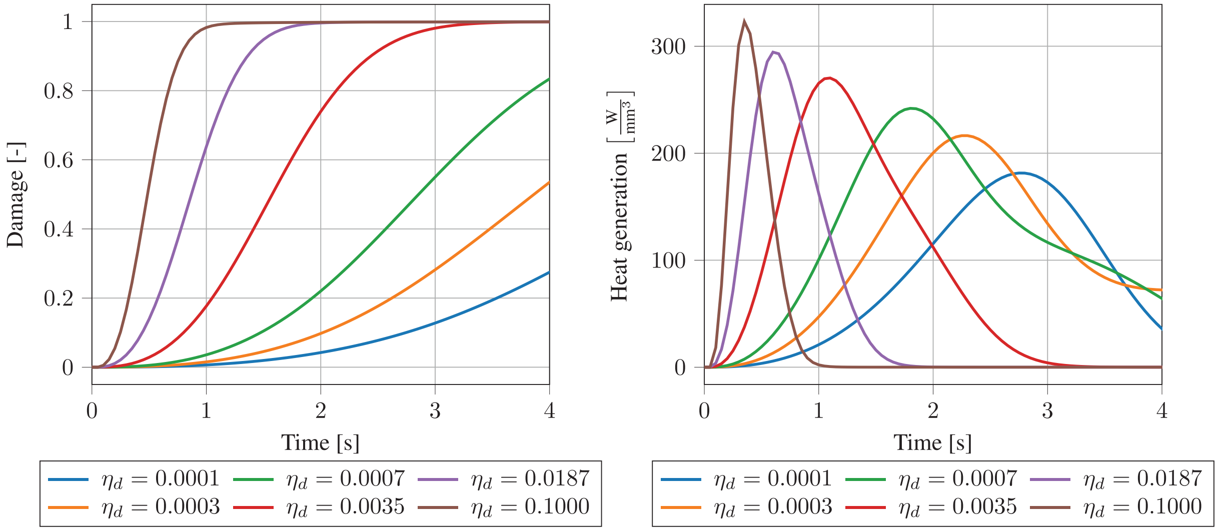

(A) Evolution of damage variable D.

(B) Evolution of internal heat source r_{int} due to damage.

FIGURE 1 Results of linear displacement applied uniaxially to a single element. Showing the influence of the damage relaxation velocity η_d.

The partial derivatives of $\mathbf{S}$, r_{int} and $\mathbf{q}_0$ with respect to the primary variables $\mathbf{C}$, $\bar{D}$ and Θ can be computed easily using *AceGen*. For the computation of the partial derivative of D with respect to $\mathbf{C}$, $\bar{D}$ and Θ we introduce $\mathbf{y} = [\hat{\mathbf{C}}, \bar{D}, \Theta]^T$ and make use of the relation

$$\Delta D = \frac{\partial D}{\partial \mathbf{y}} \Delta \mathbf{y} = -J_1^{-1} \frac{\partial r}{\partial \mathbf{y}} \Delta \mathbf{y} = \mathbf{J}_2 \Delta \mathbf{y}, \tag{18}$$

where $\hat{\mathbf{C}}$ describes the right Cauchy Green tensor in Voigt notation. The individual partial derivatives needed are then given as submatrices of the generalized Jacobian $\mathbf{J}_2$.

4 | NUMERICAL EXAMPLES

In the following section, we demonstrate the behaviour of the model described above showing some numerical studies which were conducted at integration point level. For this, an uniaxial, displacement-driven loading state with a constant loading rate is applied whilst some material parameters are varied. For the the shear modulus we chose $\mu = 30.0$ MPa whilst the bulk modulus is set to $\kappa = 1000\mu$. Furthermore, we choose a initial and reference temperature of $\Theta_a = 273.15$ K and $\Theta_0 = 273.15$ K, respectively. In all subsequent results, damage hardening is turned off, that is $k = r = 0.0$. Since we are only considering simulations on integration point level here, the gradient-extension parameters A and H as well as the heat conductivity k_0 do not have any influence. The heat capacity and the thermal expansion coefficient are chosen as $c = 2005$ Jkg^{-1}K^{-1} and $\alpha_\Theta = 10^{-3}$, respectively.

Figure 1 shows the influence of the damage velocity η_d on the evolution of damage (cf. Figure 1a) and the corresponding heat generation (cf. Figure 1b), respectively. It is clearly visible that a higher damage velocity results in a faster evolution of damage under the given boundary conditions. This effect is accompanied by a higher rate and magnitude of heat generation due to damage. Furthermore, Figure 3a shows that the total amount of heat generated is decaying with rising values of η_d. This behaviour is intuitively reasonable for the boundary value problem applied here. As the displacement is increased at a constant rate in this example, the elastic energy stored in the system increases over time. It is precisely this energy that is released as heat by damage. If the damage process takes place very quickly, there is only a small amount of energy stored in the system that can be released. In the case of a slow damage process, more displacement energy is therefore stored in the system over time and successively released through damage.

In Figure 2, we show the influence of the damage threshold Y_0 on the damage and heat generation evolution. Figure 2a shows how a higher threshold yields a later onset of damage with respect to the given loading scenario. The associated

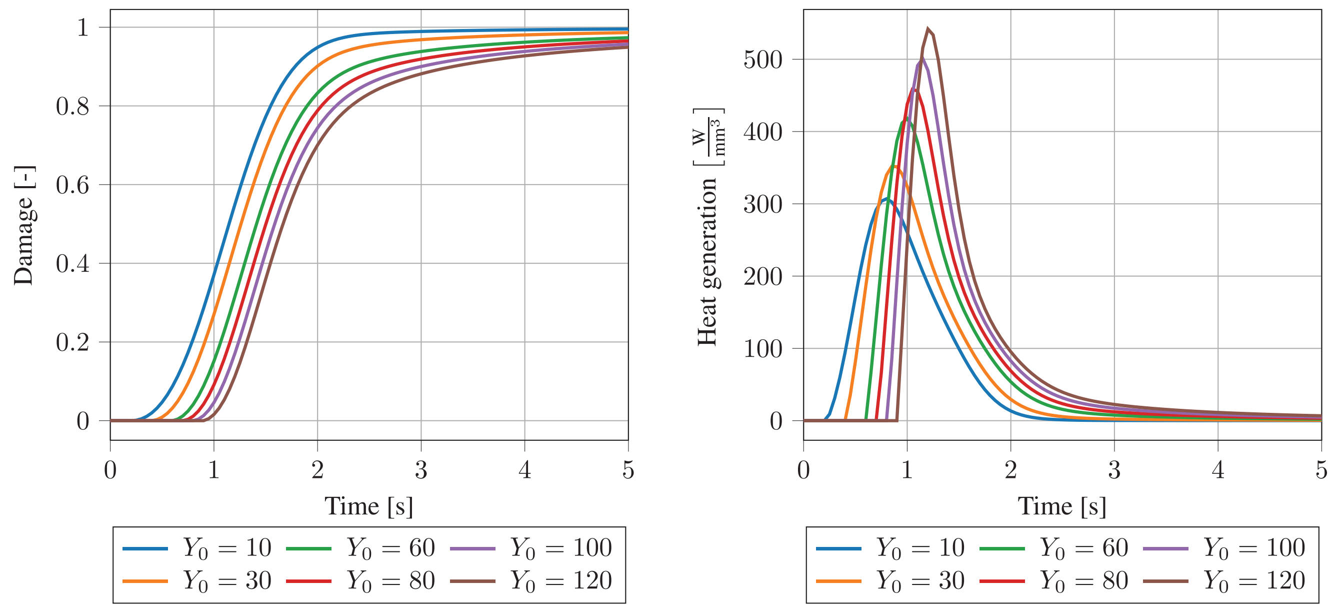

(A) Evolution of damage variable D.

(B) Evolution of internal heat source r_{int} due to damage.

FIGURE 2 Results of linear displacement applied uniaxially to a single element. Showing the influence of the damage threshold Y_0.

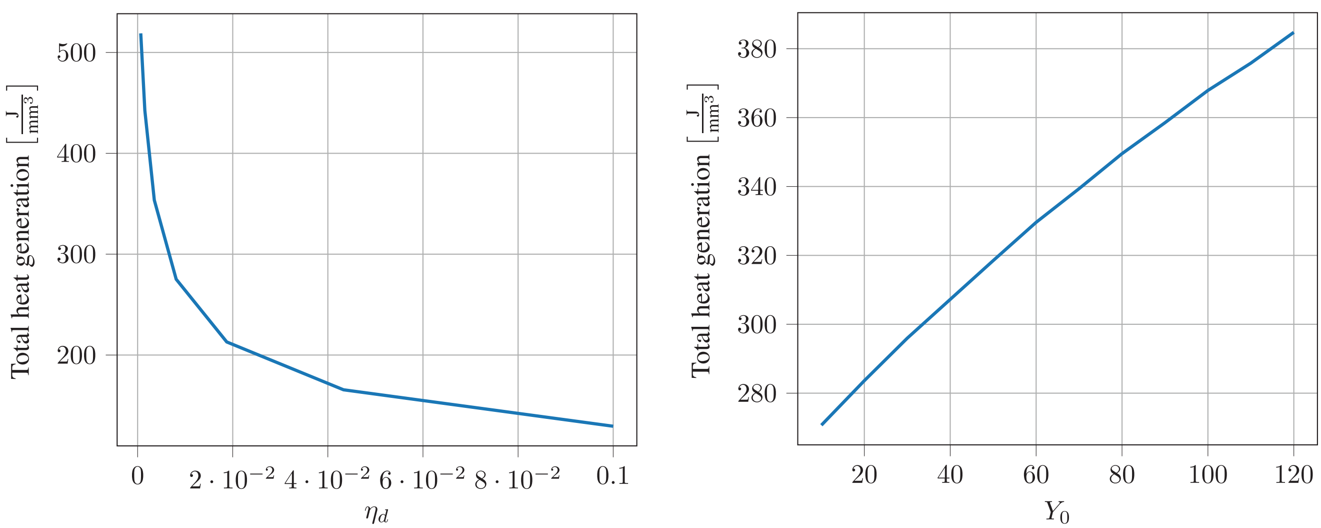

(A) Total heat generation with respect to η_d.

(B) Total heat generation with respect to Y_0.

FIGURE 3 Total heat generation for various values of damage threshold Y_0 and damage velocity η_d.

heat generation depicted in Figure 2b also shows an earlier onset for lower values of Y_0. Furthermore, it is visible that more heat get released the higher the damage threshold is set (cf. Figure 3b). Similar to the argumentation made above, this behaviour is very well expected. Since more elastic energy is already stored in the system at a later onset of the damage, correspondingly more energy is dissipated at a later onset of the damage process. This also becomes clear when looking at Equation (7), since here the heat generated depends directly on the driving force of the damage, which in turn is directly proportional to the elastic energy of the system.

Of course, the example shown here only illustrates a small part of the rate-dependent effects that the material model can reproduce. Due to the shortness of this article, other aspects, such as relaxation or creep behaviour, can unfortunately not be discussed in detail here.

5 | CONCLUSION AND OUTLOOK

In this work, we have presented an approach to modelling the thermomechanical response of rate-dependent isotropic damage within the finite deformation regime. We based our modelling approach on the well known multiplicative decomposition of the deformation gradient into mechanical and thermal parts. In order to describe the temporal evolution equations of damage, we used a Perzyna-type approach. We demonstrated the reasonability of the material response for one single use-cases of uniaxial linear deformation. These studies gave qualitatively reasonable results in both damage response and associated heat generation. Nevertheless, the model must still be investigated further with regard to other loading scenarios such as for example relaxation or creep. Furthermore, a validation using experimental data should be provided in the future. Since time-dependent damage is usually not observed as an isolated effect in real world materials, an extension of the given model with respect to other inelastic responses such as viscoelasticity must be performed in the future.

ACKNOWLEDGMENTS

Financial support by the *Arbeitsgemeinschaft industrieller Forschungsvereinigungen „Otto von Guericke" e.V.* (AiF) through the project grant IGF 21348 N/3 is gratefully acknowledged. We furthermore gratefully acknowledge the financial support provided by the *German Research Foundation* (DFG) through the projects RE 1057/45-1 (No. 403471716) and RE 1057/46-1 (No. 404502442).

Open access funding enabled and organized by Projekt DEAL.

ORCID

Lukas Lamm https://orcid.org/0000-0001-8830-6132

REFERENCES

1. Lion, A. (1997). A physically based method to represent the thermo-mechanical behaviour of elastomers. *Acta Mechanica*, *123*, 1–25.
2. Lu, S., & Pister, K. (1975). Decomposition of deformation and representation of the free energy function for isotropic thermoelastic solids. *International Journal of Solids and Structures*, *11*, 927–934.
3. Holzapfel, G. A., & Simo, J. C. (1996). Entropy elasticity of isotropic rubber-like solids at finite strains. *Computer Methods in Applied Mechanics and Engineering*, *132*, 17–44.
4. Reese, S., & Govindjee, S. (1997). Theoretical and Numerical Aspects in the Thermo-Viscoelastic Material Behaviour of Rubber-Like Materials. *Mechanics of Time-Dependent Materials*, *1*, 357–396.
5. Wulfinghoff, S., Fassin, M., & Reese, S. (2017). A damage growth criterion for anisotropic damage models motivated from micromechanics. *International Journal of Solids and Structures*, *121*, 21–32.
6. Felder, S., Kopic-Osmanovic, N., Holthusen, H., Brepols, T., & Reese, S. (2022). Thermo-mechanically coupled gradient-extended damage-plasticity modeling of metallic materials at finite strains. *International Journal of Plasticity*, *148*, 103142.
7. Lamm, L., Pfeifer, J. M., Holthusen, H., Brepols, T., & Reese, S. (2023). Modelling and Simulation of time-dependent damage and failure within silocone-based, polymeric adhesives. *Proceedings of Applied Mathematics and Mechanics*, *22*, e202200076.
8. Lamm, L., Pfeifer, J. M., Holthusen, H., Schaaf, B., Seewald, R., Schiebahn, A., Brepols, T., Feldmann, M., Reisgen, U., & Reese, S. (2023). Gradient-extended damage modelling for polymeric materials at finite strains: Rate-dependent damage evolution combined with viscoelasticity. *European Journal of Mechanics - Part A/Solids*, *103*, 105121.
9. Perzyna, P. (1963). The constitutive equations for rate sensitive plastic materials. *Quarterly of Applied Mathematics*, *20*, 321–332.
10. Voce, E. (1948). The relationship between stress and strain for homogeneous deformation. *Journal of the Institute of Metals*, *74*, 537–562.
11. Forest, S. (2009). Micromorphic Approach for Gradient Elasticity, Viscoplasticity, and Damage. *Journal of Engineering Mechanics*, *135*, 117–131.
12. Brepols, T., Wulfinghoff, S., & Reese, S. (2017). Gradient-extended two-surface damage-plasticity: Micromorphic formulation and numerical aspects. *International Journal of Plasticity*, *97*, 64–106.
13. Brepols, T., Wulfinghoff, S., & Reese, S. (2020). A gradient-extended two-surface damage-plasticity model for large deformations. *International Journal of Plasticity*, *129*, 102635.
14. Korelc, J. (2002). Multi-language and multi-environment generation of nonlinear finite element codes. *Engineering with Computers*, *18*, 312–327.
15. Korelc, J. (2009). Automation of primal and sensitivity analysis of transient coupled problems. *Computational Mechanics*, *44*, 631–649.

How to cite this article: Lamm, L., Sistig, J., Pfeifer, J. M., Holthusen, H., Felder, S., Brepols, T., & Reese, S. (2023). Modelling of damage and failure within polymeric adhesives. *Proceedings in Applied Mathematics and Mechanics*, *23,* e202300010. https://doi.org/10.1002/pamm.202300010